Chaotic probability density in two periodically driven and weakly coupled Bose-Einstein condensates

Wenhua Hai,[1,2,*] Chaohong Lee,[2] Guishu Chong,[1] and Lei Shi[2]
[1]*Department of Physics, Hunan Normal University, Changsha 410081, China*
[2]*Laboratory of Magnetic Resonance and Atomic and Molecular Physics, Wuhan Institute of Physics and Mathematics, Chinese Academy of Sciences, Wuhan 430071, China*
(Received 28 December 2001; published 6 August 2002)

Using the idea of the macroscopic quantum wave function and the definition of the classical chaos, we analytically reveal that the probability density of two periodically driven and weakly coupled Bose-Einstein condensates is deterministic but not predictable. Numerical calculation for the time evolutions of the chaotic probability density demonstrates the analytical result and exhibits the nonphysical implosions and ultimate unboundedness. A method for controlling the implosions and unboundedness is proposed through adjustment of the initial conditions that leads the probability density to periodically oscillate.

DOI: 10.1103/PhysRevE.66.026202 PACS number(s): 05.45.Ac, 03.75.Fi, 05.45.Mt, 05.30.Jp

I. INTRODUCTION

Quantum mechanics of the classically chaotic systems has been a subject of wide interest over the last few years [1–4]. However, the investigations on the dynamics of periodically perturbed one-dimensional systems demonstrated that the stochasticity of classical chaos is suppressed in the fully quantum-mechanical treatment [5,6]. This is the so-called breakdown of the correspondence principle for the chaotic systems [7,4]. Therefore, existence of the quantum chaos has become a problem of increasing interest [8]. A cause of the quantum suppression of chaos is that the classical chaos generally appears in some nonlinear systems and the corresponding quantum Schrödinger equations are linear. Therefore, a direct method for investigating the chaos associated with quantum theory is to seek a system that is nonlinear in both classical and quantum mechanics. The trapped Bose-Einstein condensates (BECs) whose quantum motions are governed by some nonlinear Schrödinger equations supply such systems for us [9].

Since the experimental observation of the Bose-Einstein condensation in a dilute gas of confined atoms [10–14], there has been much interest in the new quantum phenomena, such as the macroscopic quantum self-trapping [15,16], the quantum coherent atomic tunneling [17,18], and the physics of discrete nonlinear systems [19,20]. The chaotic behavior in two coupled BECs with periodical or kicking trapping potential have been treated [21–24]. Recently, using some direct perturbation techniques, we investigated spatiotemporal chaos and divergences of quantum-mechanical wave functions [25], and temporal chaos of quantum-mechanical phase for the superconductor Josephson junction [26]. In this paper, we will apply these results to study the inpredictability of macroscopic wave functions and exhibit the existence of chaos through two zero-temperature BECs confined in a double-well magnetic trap. The result shows that probability density of the quantum system is deterministic but not predictable. That is, the chaotic probability density contains some terms, which are analytically unsolvable and numerically uncomputable. The incomputability causes the nonphysical implosion [27] and ultimate unboundedness, and leads to the inpredictability. We call the chaos of macroscopic wave function the "macroscopic quantum chaos." By adjusting the initial conditions of the unperturbed solution, we prove that the implosion and unboundedness can be controlled such that the probability density becomes predictable periodical function.

II. CHAOTIC SOLUTION OF THE SYSTEM

Adopting the time-dependent self-consistent field method, the macroscopic one-body wave function $\Psi(\vec{r},t)$ for a weakly interacting BEC in a trap potential $V_{trap}(\vec{r},t)$ at zero temperature satisfies the Gross-Pitaevskii equation [17, 28]

$$i\hbar\frac{\partial\Psi}{\partial t}=\frac{\hbar^2}{2m}\nabla^2\Psi+[V_{trap}+g_0|\Psi|^2]\Psi, \tag{1}$$

where $g_0=4\pi\hbar^2a/m$ is the interatomic scattering pseudopotential with a and m being the atomic scattering length and mass, respectively. In order to investigate the dynamical oscillations of the isolated double-well boson Josephson junction (BJJ), we employ the time-dependent variational wave function [15,29]

$$\Psi=\psi_1(t)\Phi_1(\vec{r})+\psi_2(t)\Phi_2(\vec{r}) \tag{2}$$

with $\Phi_i(\vec{r})$ obeying

$$\int\ \Phi_i(\vec{r})\Phi_j^*(\vec{r})dr=\delta_{ij}\quad\text{for}\quad i,j=1,2 \tag{3}$$

such that the normalization condition becomes

$$\int\ |\Psi(\vec{r},t)|^2\,dr=|\psi_1|^2+|\psi_2|^2=N_1+N_2=1. \tag{4}$$

Here we have set the wave functions $\psi_i(t)=\sqrt{N_i(t)}\exp[i\theta_i(t)]$. Differing from the previous definitions,

*Email address: adcve@public.cs.hn.cn

the above wave function has been normalized so the norms $|\psi_i|^2=N_i(t)$ for $i=1,2$ are the relative occupations and $\theta_i(t)$ the phases of states. Substituting Eq. (2) into Eq. (1) and integrating over spatial coordinates reveals that $\psi_i(t)$ for $i=1,2$ are described by the nonlinear equations [17, 30, 31]

$$i\hbar\dot{\psi}_1=[E_1+U_1|\psi_1|^2]\psi_1-K\psi_2, \tag{5}$$

$$i\hbar\dot{\psi}_2=[E_2+U_2|\psi_2|^2]\psi_2-K\psi_1. \tag{6}$$

The constants E_i, U_i, and K can be written in terms of $\Phi_i(\vec{r})$ wave-function overlaps, E_1 and E_2 denote zero-point energies for each condensate; U_1 and U_2 are proportional to the mean-field energies; and K describes the tunneling dynamics between two condensates. For a time-independent parameter K, applying Eq. (4), $N_2=1-N_1$, and combining Eq. (5) with its complex conjugate produces $i\hbar\dot{N}_1=2iK\sqrt{N_1(1-N_1)}\sin(\theta_1-\theta_2)$. Defining the relative phase $\phi(t)=\theta_1(t)-\theta_2(t)$, rescaling the time to a dimensionless variable $2Kt/\hbar$ and applying $\psi_i=\sqrt{N_i(t)}\exp[i\theta_i(t)]$ to Eqs. (5) and (6), we have the set of BJJ equations,

$$\dot{N}_1=\sqrt{N_1N_2}\sin\phi=\sqrt{N_1(1-N_1)}\sin\phi, \tag{7}$$

$$\dot{\phi}=\Lambda-\Delta E-2\Lambda N_1+\frac{1-2N_1}{\sqrt{N_1(1-N_1)}}\cos\phi. \tag{8}$$

The dimensionless parameters ΔE and Λ determine the dynamic regimes of the BEC atomic tunneling and can be expressed as $\Delta E=(E_1-E_2)/(2K)+(U_1-U_2)/(4K)$ and $\Lambda=(U_1+U_2)/(4K)$. Equations (7) and (8) infer that N_1 and ϕ are the formally canonical momentum and its conjugate coordinate, which obey the formally canonical equations $\dot{N}_1=-\partial H/\partial\phi$, $\dot{\phi}=\partial H/\partial N_1$ for the conserved Hamiltonian

$$H=-\Delta EN_1-\Lambda(2N_1-1)^2/4+\sqrt{N_1(1-N_1)}\cos\phi. \tag{9}$$

The second-order derivative of N_1 can be derived from Eqs. (7)–(9) as

$$\ddot{N}_1=\frac{\partial\dot{N}_1}{\partial N_1}\dot{N}_1+\frac{\partial\dot{N}_1}{\partial\phi}\dot{\phi}=(1-2N_1)/2+(\Lambda-\Delta E-2\Lambda N_1)\times[H+\Delta EN_1+\Lambda(2N_1-1)^2/4]. \tag{10}$$

For the constant ΔE, Raghavan and coworkers gave a complicated exact solution in terms of elliptic functions [15]. When ΔE depends on time, it is quite difficult to analytically solve this equation. Therefore, in order to analyze the chaotic motion with time-dependent ΔE, we have to consider the case $|\Delta E|\ll 1$ and seek a perturbed solution. The well-known Melnikov's chaos is just the chaos of perturbed solutions [21]. To do this, we set

$$N_1=1/2+x,\quad N_2=1/2-x,\quad x=N_1-1/2=(N_1-N_2)/2 \tag{11}$$

and change Eq. (10) into

$$\ddot{x}=-(1+2\Lambda H)x-2\Lambda^2x^3-\Delta E[H+\Delta E/2+(\Delta E+\Lambda)x+3\Lambda x^2]. \tag{12}$$

The function $x(t)$ is a half of the population imbalance (N_1-N_2).

The parameters $\Delta E\neq 0$ describes the trap asymmetry. When ΔE is very small, the terms proportional to it can be regarded as perturbations to the symmetric system with $\Delta E=0$. In addition to a time-independent trap asymmetry ΔE_0, we can impose a periodically driven term into the trap asymmetry, by a small oscillation in the laser barrier position [17,32], such that

$$\Delta E=\Delta E(t)=\Delta E_0+\Delta E_1\sin\omega t\quad\text{for}\quad|\Delta E_{0,1}|\ll 1. \tag{13}$$

Application of Eq. (13) to Eq. (9) makes the latter the time-dependent Hamiltonian $H=H(N_1,\phi,t)$ with the time derivative

$$\dot{H}(t)=\frac{\partial H}{\partial t}+\frac{\partial H}{\partial N_1}\dot{N}_1+\frac{\partial H}{\partial\phi}\dot{\phi}=\frac{\partial H}{\partial t}=-\frac{d\Delta E}{dt}N_1=-\omega\Delta E_1\cos\omega t\left(x+\frac{1}{2}\right). \tag{14}$$

Integrating this equation yields

$$H(t)=H_0+H_1(t),\quad H_1(t)=-\omega\Delta E_1\int\cos\omega t\left(x+\frac{1}{2}\right)dt, \tag{15}$$

where H_0 is a constant and $H_1(t)$ a first-order small term proportional to ΔE_1. Combining Eqs. (13) and (15) with Eq. (12) result in the Duffing equation with periodical perturbations. By making use of the Melnikov-function or numerical method, chaotic oscillation of the system has been demonstrated [21,33]. In the following sections, we will use a direct perturbation approaches [24,34] to analyze the chaotic behavior of the macroscopic wave function. We expand x to first order

$$x=x_0+x_1,\quad |x_0|\gg|x_1|\sim|\Delta E|. \tag{16}$$

Here x_0 denotes the unperturbed solution and x_1 is the first-order corrections. Inserting the above expression and Eq. (15) into Eq. (12) yields the zero-order equation

$$\ddot{x}_0=-(2\Lambda H_0+1)x_0-2\Lambda^2x_0^3 \tag{17}$$

and first-order equation

$$\ddot{x}_1=-(2\Lambda H_0+1)x_1-6\Lambda^2x_0^2x_1-\varepsilon_1(t),$$

$$\varepsilon_1(t)=\Delta E(t)[H_0+\Lambda x_0(t)+3\Lambda x_0^2(t)]+2\Lambda H_1(t)x_0(t). \tag{18}$$

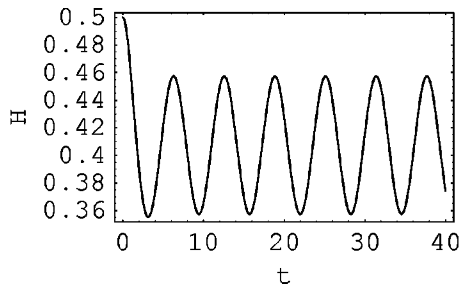

FIG. 1. Plot of the time evolutions of the dimensionless Hamiltonian $H(t)$ for the dimensionless time normalized to $\omega^{-1}=\hbar/2K$.

The unperturbed Eq. (17) has the well-known periodical solution for $(2\Lambda H_0+1)>0$ and homoclinic solution for $(2\Lambda H_0+1)<0$. We are interested in the latter associated with chaos,

$$x_0(t)=\sqrt{-(2\Lambda H_0+1)/\Lambda^2}\,\mathrm{sech}\,\xi,\quad \xi=\sqrt{-(2\Lambda H_0+1)}t+C,$$

$$C=Ar\,\mathrm{sech}[x_0(t_0)/\sqrt{-(2\Lambda H_0+1)/\Lambda^2}]-\sqrt{-(2\Lambda H_0+1)}t_0 \tag{19}$$

for $(2\Lambda H_0+1)<0$ with t_0 being the initial time. Applying Eq. (19) to Eq. (18), we construct the general solution [34]

$$x_1=x_1''\int_A^t x_1'\varepsilon_1(t)dt-x_1'\int_B^t x_1''\varepsilon_1(t)dt, \tag{20}$$

where A and B are the integration constants, x_1' and x_1'' the functions

$$x_1'=\dot{x}_0=[-(2\Lambda H_0+1)/\Lambda]\mathrm{sech}\,\xi\tanh\xi,$$

$$x_1''=x_1'\int(x_1')^{-2}\,dt=(\Lambda/2)[-(2\Lambda H_0+1)]^{-3/2}\times\mathrm{sech}\,\xi(2-3\xi\tanh\xi-\sinh^2\xi). \tag{21}$$

In the first-order approximation, using $x_0(t)$ in Eq. (19) instead of x in Eq. (15) can give the integrand of H_1 as an explicit function of time. However, the integration is analytically unsolvable. Taking the parameter set

$$H_0=0.5,\quad \Lambda=-2,\quad \omega=1,\quad \Delta E_0=\Delta E_1=0.1,$$

$$C=\pi/2,\quad A=B=0 \tag{22}$$

from Eqs. (15) we numerically plot the time evolution of $H(t)$ as Fig. 1. The curve shows the Hamiltonian tending to periodically oscillate with the increase of time. Combining Eq. (22) with Eqs. (16) and (19) we have the unperturbed population imbalance $2x_0(t)>0$ for all times, which implies the chaotic self-trapping [23,24].

Generally, the first correction (20) is unbounded, because of the unboundedness of x_1'' as time tending to infinity. However, we can easily prove that, using the l'Hôpital rule, Eq. (20) is bounded, if and only if it satisfies the condition [24,34]

$$I_\pm=\lim_{t\to\pm\infty}\int_A^t x_1'\varepsilon_1(t)dt=0. \tag{23}$$

From $I_+-I_-=0$ eliminating the constant A yields the well-known Melnikov function

$$M(t_0)=\int_{-\infty}^{\infty}x_1'\varepsilon_1(t)dt=0, \tag{24}$$

which indicates the existence of chaos and the chaotic region in parameter space [21,24]. We call the solution (20) obeying the chaos criterion (24) the "chaotic solution" [26]. Further inserting $N_1(t)$ into Eq. (7), we find the phase difference $\phi(t)$ is also chaotic. Applying the chaotic relative occupations $|\psi_1(t)|^2=N_1(t)=1/2+x$, $|\psi_2(t)|^2=N_2(t)=1/2-x$ and phase difference $\phi(t)$ to Eq. (2) leads to the corresponding chaos of the probability density $|\Psi(\vec{r},t)|^2$. Note that the chaos for the probability density comes from the definition of the classical chaos. This gives an important connection between the classical chaos and macroscopic quantum chaos. In the chaotic region of parameter space, although the probability density is deterministic for a set of fixed initial conditions and system parameters, it sensitively depends on the conditions and parameters, therefore, is unpredictable. These will be numerically illustrated in the following section.

III. INPREDICTABILITY OF THE CHAOTIC PROBABILITY DENSITY

Before computing the time evolution of probability density, it is necessary to analyze the incomputability of the chaotic solution (20). Combining Eqs. (20) and (21) with Eq. (18) we perceive that the first term of Eq. (20) insists of an unbounded function $x_1''(t)$ and an analytically unsolvable integration, which cannot be expressed as a finite form of elementary functions. To numerically give the time evolution of Eq. (20), the small deviations from the unsolvable integration are unavoidable, since any computer cannot calculate the infinite terms implied in the integration. These deviations also may come from the use of different numerical integration methods and different integration steps, even different precisions for the representation of real numbers in the computer. On the other hand, the deviations necessarily depend on the initial conditions associated with A and the system parameters. Any infinitesimal deviation will destroy the boundedness condition (23) and be amplified exponentially by the exponentially increasing function $x_1''(t)$, until infinity as $t\to\infty$. This is just the so-called sensitive dependence of chaos on the parameters and algorithm. Thus we theoretically demonstrate that the corrected solution (20) is analytically bounded but numerically unbounded, therefore uncomputable. The analytical insolvability and numerical incomputability lead to the inpredictability of the probability densities.

Applying the functions $x_0(t)$, $\varepsilon_1(t)$ and the parameters in

Eqs. (22) to Eqs. (16), (20), and (21) makes the solution the explicit form

$$x = 0.5\,\mathrm{sech}\,\xi + x_1(t),$$

$$\begin{aligned} x_1(t) = {} & 0.5\,\mathrm{sech}\,\xi(2 - 3\xi\tanh\xi - \sinh^2\xi) \\ & \times\int_0^{\xi}\mathrm{sech}\,\xi\tanh\xi[(0.1 + 0.1\cos\xi) \\ & \times(0.5 - \mathrm{sech}\,\xi - 1.5\,\mathrm{sech}^2\xi) - 2H_1(\xi)\mathrm{sech}\,\xi]d\xi \\ & - 0.5\,\mathrm{sech}\,\xi\tanh\xi\int_0^{\xi}\mathrm{sech}\,\xi(2 - 3\xi\tanh\xi - \sinh^2\xi) \\ & \times[(0.1 + 0.1\cos\xi)(0.5 - \mathrm{sech}\,\xi - 1.5\,\mathrm{sech}^2\xi) \\ & - 2H_1(\xi)\mathrm{sech}\,\xi]d\xi \end{aligned} \tag{25}$$

with variable $\xi = t + \pi/2$ and

$$H_1(\xi) = -0.05\int_0^{\xi}\sin\xi(1 + \mathrm{sech}\,\xi)d\xi. \tag{26}$$

Given Eqs. (25) and (26), we find that the first integrand in Eq. (25), namely, the integrand in Eqs. (23) and (24) is an odd function such that the boundedness condition (23) with $A = 0$ and chaos criterion (24) have been satisfied.

In Ref. [27], Saito and Ueda numerically gave the time evolution of the wave function at the origin of spatial coordinate, and showed the intermittent implosion for the trapped BECs with an attractive interaction. For the considered two-state model (2), the probability density at $\vec{r} = \vec{r}_0$ ($=$constant vector) reads

$$\begin{aligned} |\Psi(\vec{r}_0,t)|^2 = {} & |\Phi_1(\vec{r}_0)|^2|\psi_1(t)|^2 + |\Phi_2(\vec{r}_0)|^2|\psi_2(t)|^2 + \Phi_1(\vec{r}_0)\Phi_2^*(\vec{r}_0)\psi_1(t)\psi_2^*(t) + \Phi_1^*(\vec{r}_0)\Phi_2(\vec{r}_0)\psi_1^*(t)\psi_2(t) \\ = {} & |\Phi_1(\vec{r}_0)|^2 N_1(t) + |\Phi_2(\vec{r}_0)|^2 N_2(t) + \Phi_1(\vec{r}_0)\Phi_2^*(\vec{r}_0)\sqrt{N_1N_2}e^{i\phi} + \Phi_1^*(\vec{r}_0)\Phi_2(\vec{r}_0)\sqrt{N_1N_2}e^{-i\phi} \\ = {} & |\Phi_1(\vec{r}_0)|^2 N_1(t) + |\Phi_2(\vec{r}_0)|^2 N_2(t) + \sqrt{N_1N_2}\{[\Phi_1(\vec{r}_0)\Phi_2^*(\vec{r}_0) + \Phi_1^*(\vec{r}_0)\Phi_2(\vec{r}_0)]\cos\phi \\ & + [\Phi_1(\vec{r}_0)\Phi_2^*(\vec{r}_0) - \Phi_1^*(\vec{r}_0)\Phi_2(\vec{r}_0)]i\sin\phi\}. \end{aligned} \tag{27}$$

By making use of Eqs. (7), (9), (11), and (15), the probability density becomes

$$\begin{aligned} |\Psi(\vec{r}_0,t)|^2 = {} & |\Phi_1(\vec{r}_0)|^2(1/2 + x) + |\Phi_2(\vec{r}_0)|^2(1/2 - x) \\ & + [\Phi_1(\vec{r}_0)\Phi_2^*(\vec{r}_0) + \Phi_1^*(\vec{r}_0)\Phi_2(\vec{r}_0)] \\ & \times[H_0 + H_1(t) + \Delta E(t)(x + 1/2) + \Lambda x^2] \\ & + i[\Phi_1(\vec{r}_0)\Phi_2^*(\vec{r}_0) - \Phi_1^*(\vec{r}_0)\Phi_2(\vec{r}_0)]\dot{x}(t). \end{aligned} \tag{28}$$

We set $\Phi_1(\vec{r}_0) = \sqrt{R_1(\vec{r}_0)}e^{i\alpha_1}$, $\Phi_2(\vec{r}_0) = \sqrt{R_2(\vec{r}_0)}e^{i\alpha_2}$, $\alpha_1 - \alpha_2 = \alpha(\vec{r}_0)$, obtaining

$$\begin{aligned} |\Psi(\vec{r}_0,t)|^2 = {} & R_1(\vec{r}_0)(1/2 + x) + R_2(\vec{r}_0)(1/2 - x) \\ & + 2\sqrt{R_1(\vec{r}_0)R_2(\vec{r}_0)}\cos\alpha(\vec{r}_0) \\ & \times[H_0 + H_1(t) + \Delta E(t)(x + 1/2) + \Lambda x^2] \\ & - 2\sqrt{R_1(\vec{r}_0)R_2(\vec{r}_0)}\sin\alpha(\vec{r}_0)\dot{x}(t). \end{aligned} \tag{29}$$

Here the function $\dot{x}(t)$ is given by Eqs. (16), (19), and (20) as

$$\begin{aligned} \dot{x}(t) = {} & (2\Lambda H_0 + 1)\Lambda^{-1}\,\mathrm{sech}\,\xi\tanh\xi + \dot{x}_1''\int_A^t x_1'\varepsilon_1(t)dt \\ & - \dot{x}_1'\int_B^t x_1''\varepsilon_1(t)dt. \end{aligned} \tag{30}$$

When the parameter set (22) is adopted, the function $\dot{x}(t)$ denotes the time derivative of Eq. (25), namely,

$$\begin{aligned} \dot{x}(t) = {} & -0.5\,\mathrm{sech}\ \xi\tanh\xi + 0.5(3\xi\,\mathrm{sech}\,\xi - 6\xi\,\mathrm{sech}^3\xi \\ & - 6\,\mathrm{sech}\,\xi\tanh\xi - \sinh\xi) \\ & \times\int_0^{\xi}\mathrm{sech}\,\xi\tanh\xi[(0.1 + 0.1\cos\xi) \\ & \times(0.5 - \mathrm{sech}\,\xi - 1.5\,\mathrm{sech}^2\xi) - 2H_1(\xi)\mathrm{sech}\,\xi]d\xi \\ & - 0.5(\mathrm{sech}^3\xi - \mathrm{sech}\,\xi) \\ & \times\int_0^{\xi}\mathrm{sech}\,\xi(2 - 3\xi\tanh\xi - \sinh^2\xi) \\ & \times[(0.1 + 0.1\cos\xi)(0.5 - \mathrm{sech}\,\xi - 1.5\,\mathrm{sech}^2\xi) \\ & - 2H_1(\xi)\mathrm{sech}\,\xi]d\xi. \end{aligned} \tag{31}$$

The constants R_1, R_2, and α can be normalized by suitable units and may take different values that are associated with

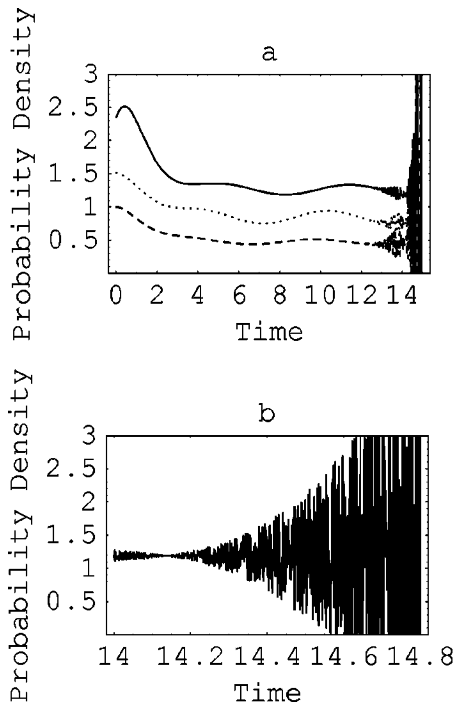

FIG. 2. Plots of the chaotic probability densities $|\Psi(\vec{r}_0,t)|^2$ versus time, which are dimensionless. The solid curve in (a) corresponds to the constants $R_1=1.5$, $R_2=0.5$, $\alpha=\pi/3$. The dashing line is associated with $R_1=1$, $R_2=0$ and the dotted line with $\alpha=\pi/2$, $R_1=1.5$, and $R_2=0.5$. These curves contain some nonphysical implosions and infinities for $t>14$, which are amplified in (b).

different $\vec{r}_0$. We shall consider the general case and several typical cases to plot the time evolutions of the probability density as follows.

Case 1: the general case. Any term of Eq. (29) does not identically vanish. Let the constants be $R_1=1.5$, $R_2=0.5$, $\alpha=\pi/3$. Substituting them and the functions $H_1(t)$ in Eq. (26) and $\Delta E(t)=0.1(1+\cos\xi)$ into Eq. (29), produces

$$\begin{aligned}|\Psi(\vec{r}_0,t)|^2 = 1.476\,314 + 0.043\,301\,3\Big[\operatorname{sech}\xi+\cos\xi(1 \\ +\operatorname{sech}\xi)-\int_0^\xi \sin\xi(1+\operatorname{sech}\xi)d\xi\Big] \\ -0.433\,013\operatorname{sech}^2(\xi)+x(\xi) \\ -1.732\,05\operatorname{sech}\xi x_1(\xi)-1.5\dot{x}(\xi),\end{aligned} \tag{32}$$

where second-order small terms have been omitted. Substituting $x(\xi)$ and $x_1(\xi)$ in Eqs. (25) and $\dot{x}(\xi)$ in Eq. (31) into Eq. (32), we employ the Mathematica to plot the solid curve of the probability density versus time in Fig. 2(a).

Case 2: a simplest case. R_1 or R_2 is zero. Setting $R_1=1$, $R_2=0$ and fixing other parameters to Eqs. (22) yields the probability density $|\Psi(\vec{r}_0,t)|^2=N_1(t)=x(t)+1/2$, which is drawn in Fig. 2(a) as the dashing line.

Case 3: $R_1\neq R_2, \cos\alpha=0$. We select the constants $\alpha=\pi/2$, $R_1=1.5$, and $R_2=0.5$, getting $|\Psi(\vec{r}_0,t)|^2=1+x(t)-1.732\,05\dot{x}(t)$. The corresponding curve of the time evolution is plotted in Fig. 2(a) as the dotted line.

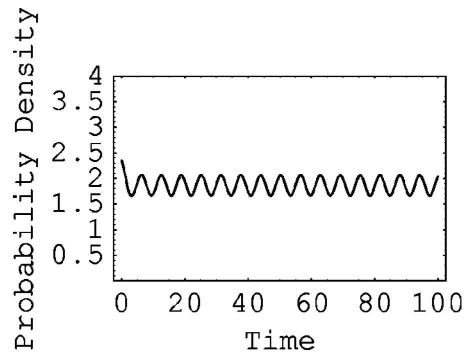

FIG. 3. Periodical oscillation of the dimensionless probability density for the coordinates $\vec{r}_0$ corresponding to the constant set $R_1=R_2=1$, $\alpha=0$.

Case 4: $R_1=R_2, \sin\alpha=0$. Taking $R_1=R_2=1$, $\alpha=0$ and omitting the second-order small terms give

$$\begin{aligned}|\Psi(\vec{r}_0,t)|^2 = 2.05+0.1\operatorname{sech}\xi-\operatorname{sech}^2\xi \\ +0.1\cos\xi(\operatorname{sech}\xi+1) \\ -0.1\int_0^\xi \sin\xi(1+\operatorname{sech}\xi)d\xi-2\operatorname{sech}\xi x_1(\xi).\end{aligned} \tag{33}$$

We plot its time evolution in Fig. 3.

The curves in Fig. 2(a) display that the probability densities of different spatial point $\vec{r}_0$ are nonperiodical for small time and occur implosions after $t=14$, and ultimately tend to infinity. Dense parts of the curves describe the implosions and show the inpredictability of the states, which are exhibited in Fig. 2(b). From Eqs. (25) and (31) we can perceive that the two integrations of them is unsolvable and the first one is multiplied by an exponentially increasing function. On the one hand, under the boundedness condition (23), the l'Hôpital rule infers the orbit (25) and (31) to be analytically bounded at an infinite time. On the other hand, in numerical computation, some unavoidable small deviations from the unsolvable integration may be exponentially amplified by the exponentially increasing function, until infinity as $t\rightarrow\infty$. This contradiction between the analytical results and numerical ones reveals that the probability density (29) with Eqs. (25) and (31) is uncomputable. The implosions and infinity of the numerical results in Fig. 2(b) are nonphysical or purely mathematical, which completely come from the numerical incomputability [8,26]. In Fig. 3 we show a quite interesting result that for some spatial coordinates $\vec{r}_0$ of case 4 the implosion and infinity disappear and the motion approaches periodical one.

Generally, the analytically unsolvable integrations implied in Eq. (29) makes the probability density the analytically unpredictable. And the implosions and infinity of numerical results lead to the numerical inpredictability of the probability density. The inpredictability of deterministic system is a basic feature of the macroscopic quantum chaos.

IV. CONTROLLING THE IMPLOSIONS AND UNBOUNDEDNESS

The probability density is an impotant quantity for the considered quantum system. An useful theory should enable us to predict it and the corresponding properties of the system. However, as we have seen that the system exists some chaotic states characterized by the implosions and unboundedness of numerical solutions, which are unpredictable. In order to theoretically predict the physical properties, we have to control the implosions and unboundedness. We shall prove that regulating the initial conditions can attain the purpose.

We recall the relationship between the initial conditions and the homoclinic solution (19) of Eq. (17). The first integration of Eq. (17) is

$$\dot{x}_0^2(t)=C_1-(2\Lambda H_0+1)x_0^2(t)-\Lambda x_0^4(t), \tag{34}$$

$$C_1=\dot{x}_0^2(t_0)-(2\Lambda H_0+1)x_0^2(t_0)-\Lambda x_0^4(t_0)$$

with t_0 being the initial time. This equation gives the homoclinic solution only for the integration constant $C_1=0$, which limits the initial values $\dot{x}_0(t_0)$ and $x_0(t_0)$ to depend on each other. Another integration constant C in the second of Eqs. (19) possesses an interesting property, namely, when the initial value $x_0(t_0)$ of the half population imbalance is equal to zero, the constant C becomes infinity for finite t_0. Now we assume that one experimentally adjusts the initial values to $\dot{x}_0(t_0)\approx 0$ and $x_0(t_0)\approx 0$ so that $C_1=0$ and $C\to\infty$. In this case, we take the parameters $H_0=0.5$, $\Lambda=-2$, $\omega=1$ such that the variable in Eqs. (19) becomes $\xi=\lim_{C\to\infty}(C+t)$. Thus we have good approximation

$$\sinh\xi\approx\lim_{C\to\infty}e^{C+t}/2,\quad \operatorname{sech}\xi\approx\lim_{C\to\infty}2e^{-(C+t)},\quad \tanh(C+t)\approx 1. \tag{35}$$

Using this approximation to Eqs. (18), (19), (20), (21), and (13) gets $x_0\approx 0$, $\varepsilon\approx H_0\Delta E(t)=0.5\Delta E(t)=0.05(1+\sin t)$ and the orbit

$$x\approx x_1\approx 0.025e^{-t}\int_B^t e^t(1+\sin t)dt-0.025e^t\times\int_A^t e^{-t}(1+\sin t)dt,$$

$$\dot{x}\approx\dot{x}_1\approx -0.025e^{-t}\int_B^t e^t(1+\sin t)dt-0.025e^t\times\int_A^t e^{-t}(1+\sin t)dt. \tag{36}$$

Obviously, boundedness of the solution needs $A=\infty$ and B being finite. Setting $A=\infty$, $B=0$, Eqs. (36) represent a periodical orbit. Inserting such $x(t)$, $\dot{x}(t)$, and Eqs. (15), $H_1\approx -0.05\sin t$, into Eq. (29) and selecting $R_1=1.5$, $R_2=0.5$, $\alpha=\pi/3$ of the general case, we arrive at

$$|\Psi(\vec{r}_0,t)|^2=1.476\,314+x(t)-1.5\dot{x}(t)$$
$$=1.476\,314+0.0625e^{-t}\int_0^t e^t(1+\sin t)dt+0.0125e^t\int_\infty^t e^{-t}(1+\sin t)dt. \tag{37}$$

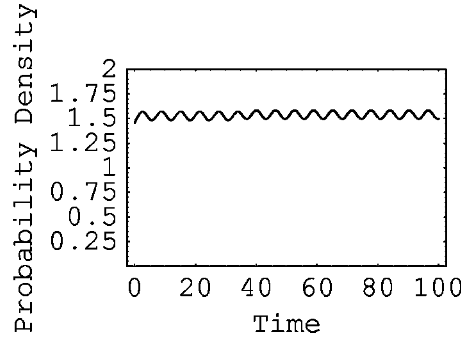

FIG. 4. Periodical oscillation of the dimensionless probability density versus dimensionless time for the initial conditions $\dot{x}_0(t_0)\approx 0$, $x_0(t_0)\approx 0$ and the constants $R_1=1.5$, $R_2=0.5$, $\alpha=\pi/3$, where the implosions and infinities have been controlled.

This is also a periodical function of time that has been numerically illustrated in Fig. 4. The periodical oscillation of the probability density is predictable. Thus we have controlled the implosions and unboundedness, through the adjustments of the initial conditions. Knowing Eqs. (11) and (16), the considered initial conditions $\dot{x}_0(t_0)\approx 0$ and $x_0(t_0)\approx 0$ means that $N_1(t_0)\approx N_2(t_0)$ and $\dot{N}_1(t_0)\approx\dot{N}_2(t_0)\approx 0$, that is, initially, the unperturbed particle numbers in each trap to be approximately same and invariable. Therefore, if one can realize such initial conditions experimentally by adjusting the system, the macroscopic quantum chaos will be suppressed.

V. CONCLUSION

In summary, we have studied the macroscopic quantum chaos of two zero-temperature BEC confined in a double-well magnetic trap. Using the time-dependent self-consistent field method and the macroscopic one-body wave function, we investigated the BJJ equations that describe time evolutions of the relative occupations and phase difference. Under the Melnikov criterion of classical chaos, we find the chaotic quantum system possessing deterministic but unpredictable probability density. That is, the probability density is analytically bounded but numerically unbounded, and the numerical result appears the nonphysical implosions and unboundedness. This makes the system the analytically unsolvable and numerically uncomputable, which result in the theoretical inpredictability of the chaotic probability density.

It is clear that although a regular quantum system must be made probability interpretation, the corresponding probability is deterministic and predictable. However, the chaotic quantum systems not only need probability interpretation but also the corresponding probability is unpredictable. According to the general definition, chaos is merely a synonym for randomness of the deterministic systems [8]. The above result shows that the macroscopic quantum motion with random probability density is an essential feature of the macroscopic quantum chaos. To theoretically predict the macroscopic quantum states, we suggest a method for controlling the nonphysical implosions and unboundedness, namely, regulating the initial conditions to make the chaotic solution the periodical one.

ACKNOWLEDGMENTS

This work was supported by the NNSF of China under Grant No. 19874019, the Laboratory of Magnetic Resonance and Atomic and Molecular Physics of China under Grant No. T152103, and the Hubei Provincial Key Laboratory of Gravitation and Quantum Physics of China.

[1] M. Gutzwiller, *Chaos in Classical and Quantum Mechanics* (Springer, Berlin, 1990).
[2] Y. Gu, *Quantum Chaos* (Scientific and Technological Education Press, Shanghai, 1996).
[3] S. Chaudhuri, G. Gangopadhyay, and D. S. Ray, Phys. Lett. A **216**, 53 (1996).
[4] B. S. Helmkamp and D. A. Browne, Phys. Rev. Lett. **76**, 3691 (1996).
[5] T. Hogg and B. A. Huberman, Phys. Rev. Lett. **48**, 711 (1982).
[6] B. Sundaram and P. W. Milonni, Phys. Rev. E **51**, 1971 (1995).
[7] R. Roncaglia, L. Bonci, B. J. West, and P. Grigolini, Phys. Rev. E **51**, 5524 (1995).
[8] J. Ford, in *The New Physics*, edited by P. Davies (Cambridge University Press, Cambridge, 1989), p. 348.
[9] A. J. Leggett, Rev. Mod. Phys. **73**, 307 (2001).
[10] M. H. Anderson, J. R. Ensher, M. R. Matthews, C. E. Wieman, and E. A. Cornell, Science **269**, 198 (1995).
[11] K. B. Davis, M. O. Mewes, M. R. Andrews, N. J. van Druten, D. S. Durfee, D. M. Kurn, and W. Ketterle, Phys. Rev. Lett. **75**, 3969 (1995).
[12] K. B. Davis, M. O. Mewes, and W. Ketterle, Appl. Phys. B: Lasers Opt. **B60**, 155 (1995).
[13] C. C. Bradley, C. A. Sackett, J. J. Tollett, and R. G. Hulet, Phys. Rev. Lett. **75**, 1687 (1995).
[14] M. R. Andrews, C. G. Townsend, H. J. Miesner, D. S. Durfee, D. M. Kurn, and W. Ketteerle, Science **275**, 637 (1997).
[15] S. Raghavan, A. Smerzi, S. Fantoni, and S. R. Shenoy, Phys. Rev. A **59**, 620 (1999).
[16] L. M. Kuang and Z. W. Ouyang, Phys. Rev. A **62**, 023610 (2000).
[17] A. Smerzi, S. Fantoni, S. Giovanazzi, and S. R. Shenoy, Phys. Rev. Lett. **79**, 4950 (1997).
[18] B. Hu and L. M. Kuang, Phys. Rev. A **61**, 023604 (2000).
[19] F. S. Cataliotti, S. Burger, C. Fort, P. Maddaloni, F. Minardi, A. Trombettoni, A. Smerzi, and M. Inguscio, Science **293**, 843 (2001).
[20] A. Trombettoni and A. Smerzi, Phys. Rev. Lett. **86**, 2353 (2001).
[21] F. Kh. Abdullaev and R. A. Kraenkel, Phys. Rev. A **62**, 023613 (2000).
[22] S. A. Gardiner, D. Jaksch, R. Dum, J. I. Cirac, and P. Zoller, Phys. Rev. A **62**, 023612 (2000).
[23] P. Coullet and N. Vandenberghe, Phys. Rev. E **64**, 025202(R) (2001).
[24] C. Lee, W. Hai, L. Shi, X. Zhu, and K. Gao, Phys. Rev. A **64**, 053604 (2001).
[25] W. Hai, M. Feng, X. Zhu, L. Shi, K. Gao, and X. Fang, J. Phys. A **32**, 8265 (1999); Phys. Rev. A **61**, 052105 (2000); J. Phys. A **34**, L79 (2001).
[26] W. Hai, X. Liu, J. Fang, X. Zhang, W. Huang, and G. Chong, Phys. Lett. A **275**, 54 (2000); W. Hai, Y. Xiao, J. Fang, W. Huang, and X. Zhang, *ibid.* **265**, 128 (2000); W. Hai, X. Zhang, W. Huang, and G. Chong, Int. J. Bifurcation Chaos Appl. Sci. Eng. **11**, 2263 (2001).
[27] H. Saito and M. Ueda, Phys. Rev. Lett. **86**, 1406 (2001).
[28] E. P. Gross, Nuovo Cimento **20**, 454 (1961); J. Math. Phys. **4**, 195 (1963).
[29] I. Marino, S. Raghavan, S. Fantoni, S. R. Shenoy, and A. Smerzi, Phys. Rev. A **60**, 487 (1999).
[30] M. J. Steel and M. J. Collett, Phys. Rev. A **57**, 2920 (1998).
[31] Chi-Yong Lin, E. J. V. de Passos, and D. S. Lee, Phys. Rev. A **62**, 055603 (2000).
[32] A. Smerzi and S. Raghavan, Phys. Rev. A **61**, 063601 (2000).
[33] G. Hu and Z. Qu, Phys. Rev. Lett. **72**, 68 (1994).
[34] W. Hai, Y. Duan, and L. Pan, Phys. Lett. A **234**, 198 (1997).